Hindawi
Geofluids
Volume 2021, Article ID 6629237, 9 pages
https://doi.org/10.1155/2021/6629237

Research Article

Experimental Research on Permeability of Coal and Rock Mass considering Postpeak Failure

Zhiguo Cao,[1] Hualei Zhang ,[1,2] Jiadi Yin,[2] and Baojie Fu[2]

[1]*State Key Laboratory of Water Resource Protection and Utilization in Coal Mining, Beijing 100120, China*
[2]*Key Laboratory of Safe and Effective Coal Mining of the Ministry of Education, Anhui University of Science and Technology, Huainan 232001, China*

Correspondence should be addressed to Hualei Zhang; hlzhang1122@126.com

Received 23 December 2020; Revised 13 January 2021; Accepted 8 February 2021; Published 22 March 2021

Academic Editor: Feng Xiong

Copyright © 2021 Zhiguo Cao et al. This is an open access article distributed under the Creative Commons Attribution License, which permits unrestricted use, distribution, and reproduction in any medium, provided the original work is properly cited.

In most mining areas of China, coal seams are characterized by low gas pressure, poor permeability, and high gas adsorption capacity, all of which have brought considerable difficulties to coal seam mining and coalbed methane (CBM) extraction. According to the multiyear scientific research and production practice of China, gas is migrated in quantity only after the coal body is directly mined, and the surrounding rocks deform and fracture under the mining influence. Thus, the key to effective control of gas migration and the coal and CBM comining technology lies in investigating the gas resolution, permeation, migration, and accumulation laws in the coal seams under the unloading confining pressure during mining. The MTS815.02 rock mechanics testing system and its supporting equipment are combined to test the permeability characteristics of coal and rock mass (postpeak fractured coal and sandstone specimens) under the loading and unloading of confining pressure using the steady method, and then, the permeation laws of the fractured coal and rock mass are obtained. Results show that after the postpeak rock crack propagation reaches a stable state, the confining pressure gradually increases, and the gas permeability presents an approximately linear reduction; in the postpeak unloading phase, the opening and coalescence degree of rock cracks gradually increase as the deformation extends. Thus, permeability reaches a peak value. The strain softening phase follows, where the cracks are closed and permeability declines to a certain extent. Moreover, the unloading step size of confining pressure has bearing on gas permeability. Specifically, as the unloading step size of confining pressure decreases, the change of gas permeability increases in stability.

1. Introduction

As burial depth increases, gas pressure at the coal seam progressively increases at the hydrostatic pressure gradient. The gas pressure and content increase with the coal mining depth, and the gas disaster also increases in severity. From the perspective of safety mining, gas should be first extracted and coal mining follows. However, the gas occurrence in most coal mining areas of China is characterized by low permeation pressure, low saturability, and especially, low permeability and strong heterogeneity. As a result, ground gas preextraction technique faces many difficulties. In two mining areas, namely, Huainan and Huaibei, the working seams have highly complicated structures, metamorphic degree of coal seam ranges from long flame coal to anthracitic coal, gas content reaches 10–30 m^3/t, Protodyakonov coefficients of coal are mostly within 0.1–0.4, and the coal seam permeability is only 10^{-7}–10^{-6} [1]. The latter differs from the coal seam permeability in the San Juan Basin of America by 10^4–10^5 times, and this difference is the primary cause for the difficult gas extraction before coal mining in most mining areas of China. Theoretical research and engineering practice suggest that the technical route of underground mining under unloading confining pressure, and safe and efficient coal and gas comining, should be taken in most low-permeability coal mining areas [2, 3].

Gas-containing coal is a multiphase porous fractured medium that contains different contents of gas, such as methane. With coal seam mining, the coal and rock mass undergoes a stress redistribution that results in its

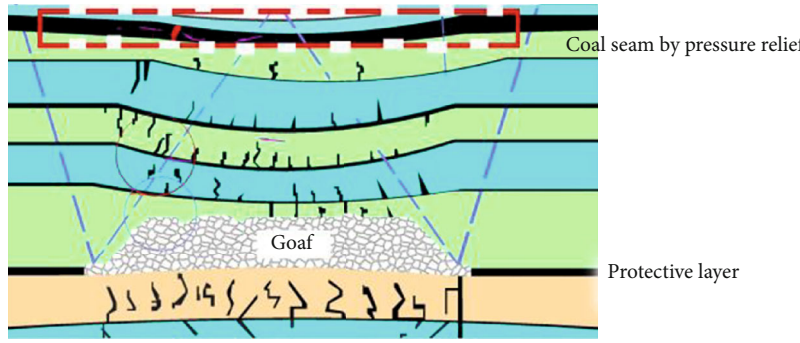

Figure 1: Schematic diagram of mining under pressure relief.

deformation and failure. A large number of secondary cracks are generated, and its gas permeability changes, which lead to gas resolution and flow [4–6].

Coal and rock mass is a porous fractured medium with a highly complicated structure. The crack distribution characteristics are also complicated, and permeability shows heterogeneity and anisotropy under the mining influence. Meanwhile, permeability is closely related to the pore structure of coal rock, deformation and failure characteristics [7–13], mining ground pressure, gas pressure at coal seam, gas adsorption, and resolution characteristics. During mining, the gas migration state changes under the pressure relief condition of the coal seam, as shown in Figure 1. Mining practice indicates that the ground pressure plays a critical role in the permeability change of coal seam, while permeability exerts a very important effect on gas accumulation, outburst, and pressure distribution. The change of stress environment has a great bearing on the coal permeability at constant temperature [14–18]. However, the quantitative relationship between loading and unloading of confining pressure and permeability when the coal and rock mass reaches its peak value but does not enter the crushed state has not been measured. That is, the seepage characteristics of the upper and low rock (coal) masses at the pressure-relieved coal seam after bearing the mining influence have not been investigated. Therefore, probing the gas permeability change in postpeak coal and rock mass presents a considerable guiding significance to coalbed methane (CBM) extraction under pressure relief conditions. This study mainly explores the permeability characteristics of postpeak coal and rock specimens under loading and unloading conditions of confining pressure.

2. Test Preparation

2.1. Testing System. The testing system was divided into two parts: gas permeability control and electrohydraulic servo-controlled rock mechanics testing system (MTS). The liquid permeation inlet and outlet in the MTS testing system were transformed and docked with the gas inlet and outlet in the gas permeation control, and then, the rock gas permeability test was carried out under confining pressure. These two parts of the testing system are stated below. Figure 2 shows the MTS815.02 electrohydraulic servocontrolled rock mechanics testing system.

Figure 3 shows the entire set of the rock gas permeability testing system under confining pressure and its working principles. Figure 4 shows the principles of the rock gas permeability test under unloading confining pressure.

2.2. Preparation of Rock Specimens. Postpeak rock specimens were obtained by applying axial displacement (3 mm) to all rock specimens (sandstone and coal are commonly used in engineering practice) selected in this test after loading to a peak value and experiencing failure. For comparability of test results, all rock specimens with the same lithology were collected from the same location. The rock specimens had a diameter and height of 50 mm (error: ±2 mm) and 100 mm (error: ±2 mm), respectively.

The processed standard rock specimens were applicable to the MTS triaxial testing system only after sealing with PVC insulated rubber tape and two thermal shrinkage plastic packages. The rock specimens prepared for the test are shown in Figures 5 and 6.

3. Test Method

In the laboratory, the rock permeability coefficient or permeability is determined using various testing apparatuses and methods, most of which can be classified into the steady-state and transient methods [19–23].

The steady-state method is also called the normal pressure method, namely, measuring the flow quantity under a fixed pressure head and then calculating the permeability coefficient. The transient method is also called the pulse decay method, where the attenuation of waterhead difference at two ends of the rock specimen within a certain period is determined to calculate the permeability coefficient.

The transient method is suitable for determining low-permeability rock specimens. Therefore, in this test, the steady-state method is used to determine the permeability of rock specimens. The procedures are adopted as follows. A certain axial load P_1 and confining pressure P_2 (passive confining pressure in the permeameter) are first applied to each rock specimen, and the rock gas permeability testing system begins [24]. The gas outlet is closed while the gas inlet is opened, and thus, all pipelines from the rock specimen are filled with constant-pressure gas. Subsequently, the gas outlet is reopened to form the permeation pressure difference ΔP at the two ends of the specimen, allowing the gas to seep

Figure 2: MTS815.02 electrohydraulic servocontrolled rock mechanics testing system.

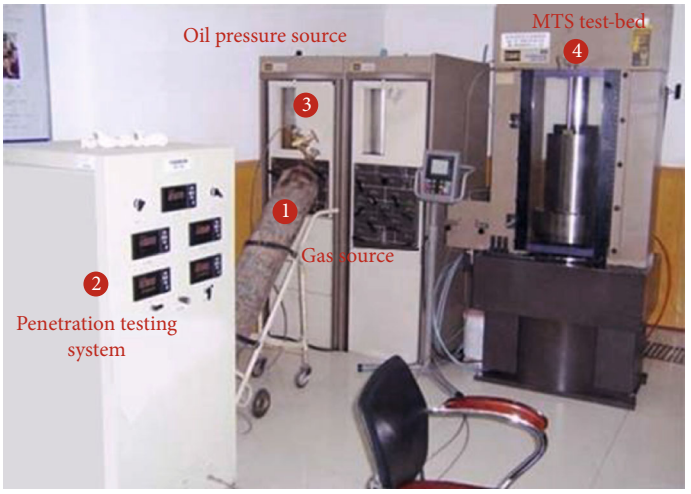

Figure 3: Rock gas permeability testing system.

through. When ΔP became constant, the inlet pressure, pressure difference, and flow quantity are recorded. Under the same conditions, inlet pressure is changed to test another group of data. The permeability of the rock specimen under the present conditions can be obtained according to the following formulas (1)–(6).

In reality, seepage in the fractured rock mass is not a Darcy flow in the strict sense. By combining the characteristics of the testing system and its output variables, the calculation formula of permeability and its derivation are as follows.

The pressure gradient and seepage velocity of 1D non-Darcy seepage satisfy the below relationship:

$$\frac{dp}{dx} = -\left(\frac{\mu}{k}V + \beta\rho V^2\right). \tag{1}$$

Equation (1) is also called the Forchheimer equation [25], where dp/dx is the crack pressure gradient (MPa/m), V is seepage velocity (m/s), μ is aerodynamic viscosity (Pa·s), k is permeability (μm^2), ρ is mass density (kg/m^3), and β is non-Darcy flow permeability factor (m^{-1}).

The integral is taken from Equation (1) along the length L of the seepage specimen to obtain the following:

$$\frac{P_1 - P_2}{L} - \beta\rho V^2 = \frac{\mu V}{k}, \tag{2}$$

where P_1 is inlet pressure and P_2 is outlet pressure.

Q_1 is set as the flow quantity under $\lambda(P_1 + P_2)$; Q_2 is flow quantity at the outlet. The following can be obtained according to the gas state equation [104]:

$$Q_1 = \frac{P_2 Q_2}{\lambda(P_2 + P_1)}, \tag{3}$$

where λ is a positive factor. Equation (3) is substituted into Equation (2), and in consideration of $Q_1 = A \cdot V$ (A is cross-

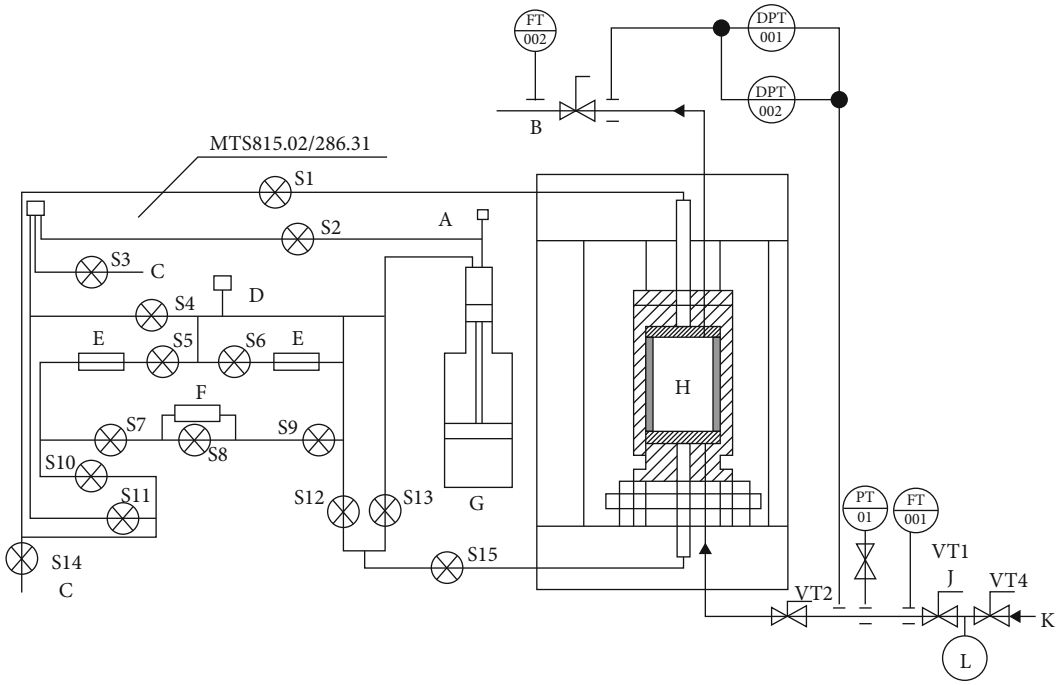

Figure 4: Schematic diagram of rock gas permeability test under unloading confining pressure.

Figure 5: Rock specimen placed on MTS815 system.

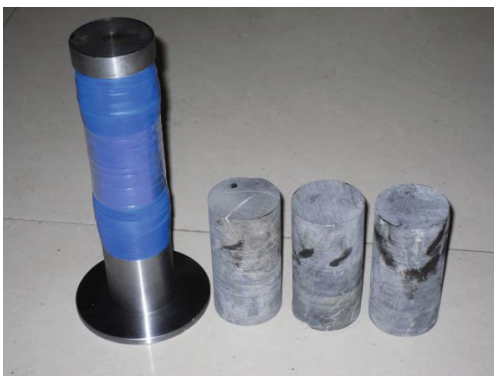

Figure 6: Postpeak rock specimen for measurement.

sectional area of seepage flow), permeability k can be solved as

$$k = \frac{1}{\left(P_1^2 - P_2^2\right)\lambda A/\mu P_2 Q_2 L - \beta\rho P_2 Q_2/\lambda A\mu(P_1 + P_2)}. \quad (4)$$

International units are taken for the variables at the right side of the equation, and the unit of k is derived as m^2.

The inlet pressure P_3 and outlet pressure P_4 of the specimen are changed, and the flow quantity Q_4 at the outlet is measured, and thus, a relational expression similar to Equation (4) can be obtained:

$$k = \frac{1}{\left(P_3^2 - P_4^2\right)\lambda A/\mu P_4 Q_4 L - \lambda\beta\rho P_4 Q_4/A\mu(P_3 + P_4)}. \quad (5)$$

The β factor of non-Darcy flow under the test conditions can be obtained by comparing Equations (4) and (5):

$$\beta = \frac{\left(P_1^2 - P_2^2\right)\lambda^2 A/\rho P_2 Q_2 L - \left(P_3^2 - P_4^2\right)\lambda^2 A/\rho P_4 Q_4 L}{P_2 Q_2 (P_3 + P_4) - P_4 Q_4 (P_1 + P_2)/A(P_1 + P_2)(P_3 + P_4)}. \tag{6}$$

The β factor solved through the above equation is substituted into Equations (4) or (5) to obtain the permeability k. International units are taken for the variables at the right side of Equation (6), and the unit of β is derived as m^{-1}.

If the factor is expressed by the permeability coefficient, the following substitution can be carried out:

$$K = \frac{k\gamma}{\mu} = \frac{kg}{\nu}, \tag{7}$$

where μ and υ are dynamic and kinematic viscosity, respectively, and γ is proportion. The unit of υ is derived as m^2/s, and the unit of γ is derived as N/m^3.

The rock permeability is determined via testing. After the test at the first experimental point is completed, its parameters can be adjusted to start that of the next experimental point. Under the load control mode of the servo, the permeability values under different stress states can be measured by continuously increasing the axial load or continuously unloading the confining pressure. When the specimen is a postpeak rock, the load control mode can easily cause the machine to go out of control. Therefore, switching into the displacement control mode is necessary. Based on the above idea, Figure 7 shows the program chart of the MTS rock permeability test under confining pressure.

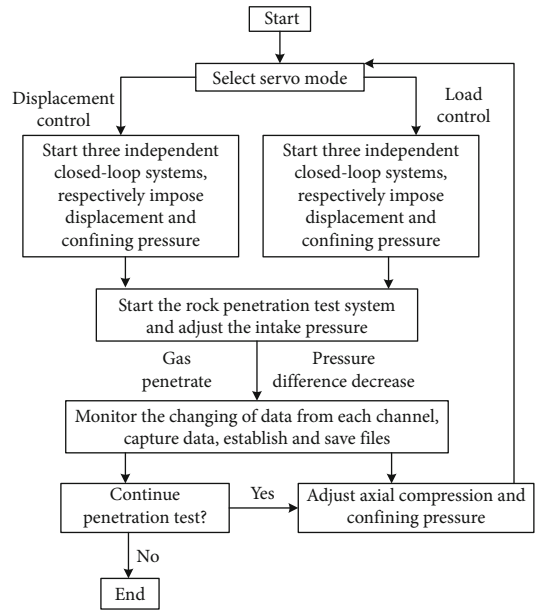

Figure 7: Control flow chart of permeability test under unloading confining pressure.

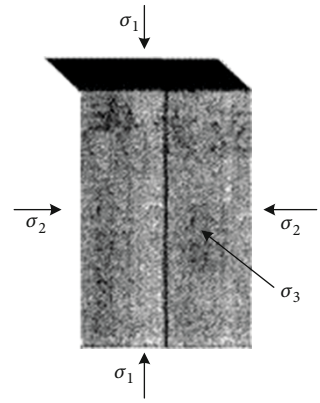

Figure 8: Crack permeation model.

4. Analysis of Test Results

4.1. Gas Permeability of Postpeak Rock under the Unloading Confining Pressure. The gas source in this test is nitrogen with basic parameters of $\mu = 0.176 \times 10^{-4}$ Pa · s and $\rho = 1.16$ kg/m^3. The inlet pressure, outlet pressure, flow quantity at outlet, and permeability of each rock specimen are recorded during the unloading confining pressure test.

4.1.1. Influence of Unloading Confining Pressure on Gas Permeability of Postpeak Rock. With the rock unloading, the cracks in the fractured rock also change, which can be divided into the two following circumstances.

Circumstance 1. As the confining pressure is unloaded, the cracks in the postpeak fractured rock continuously expand. With continuous gas permeation, the crack expansions accelerate, permeability continuously increases, and the variation trend also accelerates.

Circumstance 2. In consideration of the crack development in postpeak rock, σ_2 and σ_3 (Figure 8) gradually decrease with the unloading of confining pressure. Small broken pieces generated during the crack development block the gradually expanded rock cracks in the axial direction due to the acting force of σ_1 and pressure at the inlet. Thus, the gas permeability of the rock suddenly decreases.

Through the experimental study, Figures 9 and 10 show the change curves of the gas permeability of rock specimens with different lithologic characteristics during the unloading of confining pressure under constant axial displacement (displacement control is commonly axial in the MTS).

Figure 11 presents the confining pressure-permeability change curve of sandstone. The relation graph shows that the confining pressure starts unloading from 5 MPa, and permeability continuously increases with the unloading quantity. In the initial unloading phase, permeability changed little, and the unloading velocity of confining pressure is basically in direct proportion to the growth of permeability. When the confining pressure of sandstone unloads from 3 to 2 MPa, permeability changes considerably. Clear change

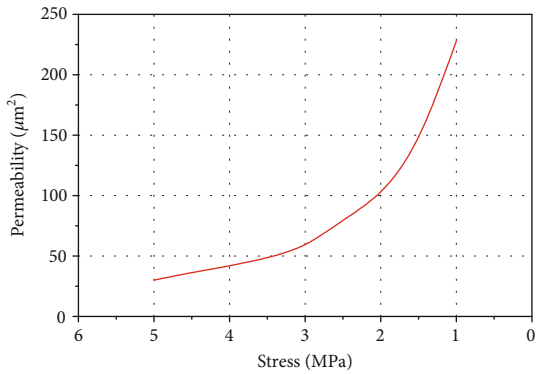

Figure 9: Change curve of permeability with confining pressure for the coal specimen 1.

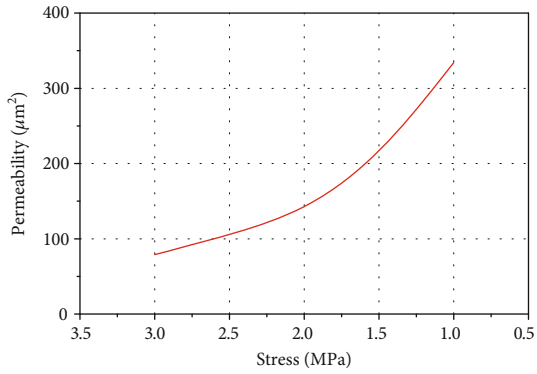

Figure 10: Change curve of permeability with confining pressure for the coal specimen 2.

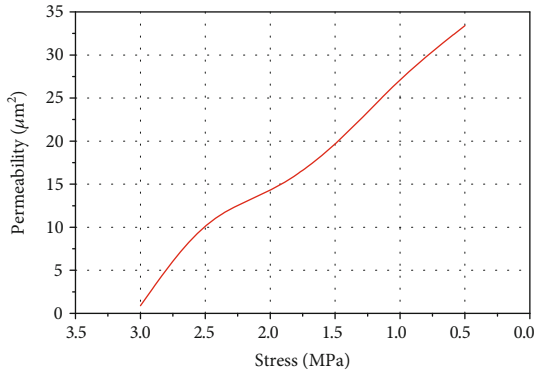

Figure 11: Confining pressure-permeability change curve of coal specimen 2.

points appear in the permeability curve, indicating that microcracks induced in the sandstone gradually propagate and penetrate to form a thorough crack passage. With the reduction of confining pressure, the crack development clearly increases under the action of axial load, gas flow is not characterized by slow diffusion, and the seepage flow generated by the gas through the pores has a much weaker influence relative to the flow velocity of the gas in the cracks.

Table 1: Main technical specifications.

Axial load	<1700 kN
Confining pressure	<45 MPa
Pore water pressure	<45 MPa
Stiffness of load frame	10.5×10^9 N/m
Capacity of hydraulic power source (HPS) motor	18 kW
Sensitivity of servo valve	290
Number of data channels (Chans. data acquisition)	10 chans
Minimum sampling time (Min. sampling time)	50 μs
Maximum specimen diameter (maximum diameter of similar equipment introduced in China)	100 mm
Maximum specimen height	200 mm

Figures 9 and 10 show the confining pressure-permeability change curves of the coal specimen. Due to the low strength of coal, the confining pressure started unloading from 3 MPa, and the unloading velocity was 1 MPa per step. Compared with coal, the greatest difference of sandstone is that clear change points appeared from the start of unloading confining pressure until its completion, and the permeability apparently enlarged. However, the slopes of permeability change curves of coal from the commencement to completion of unloading were approximate, indicating that the postpeak crack development in coal is evidently better, and therefore, permeability change was also clearer, than that in sandstone. In consideration of coal brittleness during the loading of initial confining pressure, new cracks might expand based on the original ones under the axial load.

4.1.2. Influence of Unloading Step of Confining Pressure on Postpeak Gas Permeability. From the test data, the gas permeability values of both sandstone and coal rock specimen under the postpeak unloading condition of confining pressure show obvious changes. The unloading of confining pressure exerts a highly significant influence on permeability, which is analyzed in terms of the unloading step size of confining pressure, as seen in Table 1.

The following deductions can be obtained from Table 2. The unloading of confining pressure in coal and rock specimens causes considerable permeability change. In comparison with sandstone, coal shows a large change in permeability since unloading confining pressure started until completion. The maximum change can reach two orders of magnitude, while that of sandstone is relatively smaller, indicating that the permeability of overlying coal mass was higher than that of rock under the unloading of confining pressure.

Compared with coal specimens 1 and 2, coal specimen 3 clearly has lower unloading velocity of confining pressure. In addition, in the initial unloading phase of confining pressure, coal specimen 3 has steady gas permeability. The sudden increase or reduction of permeability does not occur easily. Therefore, as the unloading step size of confining pressure decreases, the stability of permeability change increases.

Table 2: Gas permeability test data and calculation results.

Specimen	Unloading step size	Permeability at different confining pressures ($\times 10^{-5}$ m^2)				
		5 MPa	4 MPa	3 MPa	2 MPa	1 MPa
Sandstone 1	1.0 MPa	0.68	1.14	1.70	2.25	4.83
Coal specimen 1	1.0 MPa	$6.53E-11$	$8.33E-11$	0.97	1.06	5.22
Sandstone 2	0.5 MPa	3.01	4.17	5.72	9.95	22.8
Coal specimen 2	0.5 MPa	$6.67E-12$	$1.67E-11$	0.09	1.38	2.75
Coal specimen 3	0.3 MPa	$6.20E-12$	$3.62E-11$	2.62	7.23	29.5

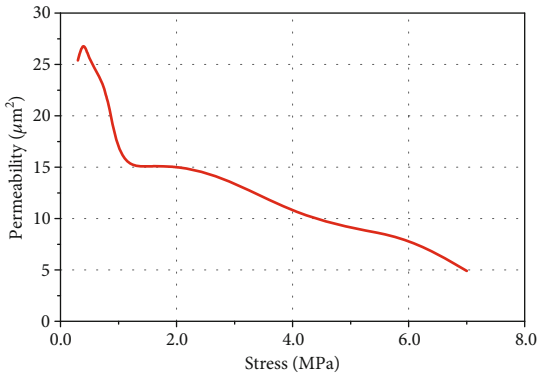

Figure 12: Permeability change curves of rock specimen 3 under loading of confining pressure.

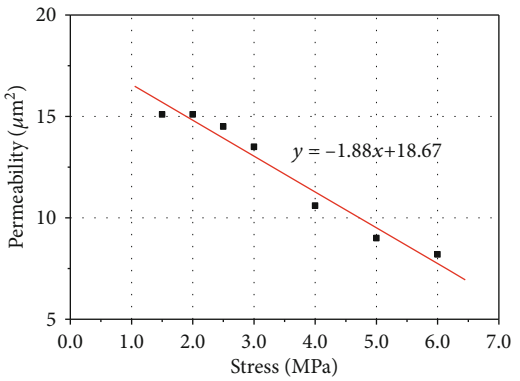

Figure 13: Permeability scatter diagram of rock specimen 3.

4.2. Gas Permeability of Postpeak Rock Specimen under Loading Confining Pressure. Under the mining influence in engineering practice, besides the postpeak unloading of confining pressure, the stress concentration area is usually generated after the unloading of confining pressure, and the rock bears the increasing load. For this reason, the change of rock gas permeability is analyzed under the postpeak loading confining pressure by taking sandstone as the study object. Figure 12 shows the test data organized to obtain the increasing confining pressure-permeability change curves.

Figure 12 shows that the circumferential stability of the rock specimen is relatively maintained due to the action of small confining pressure, while only a few cracks develop as influenced by the axial force. Thus, small bulges appear at the beginning. With the gradual increase of confining pressure, specifically under 0.5 MPa in this test, the permeation conditions clearly change. The permeability considerably changes from 0.8 to 1 MPa. As the confining pressure increases to 1 MPa, the confining pressure has a clear effect on the cracks, which is most directly manifested by the sudden reduction of permeability and at a significant decrease in amplitude. The possible explanation is that when the confining pressure reaches 1 MPa, the confining pressure leads to the sudden closure of large cracks in the rock specimen and further causes the sudden decrease of permeability.

When the confining pressure loads from 1 to 7 MPa, the permeability change of the rock specimen becomes steadier than that in the early stage. Figure 13 shows that the scatter diagram is fitted according to the relationship between permeability and confining pressure after 1 MPa.

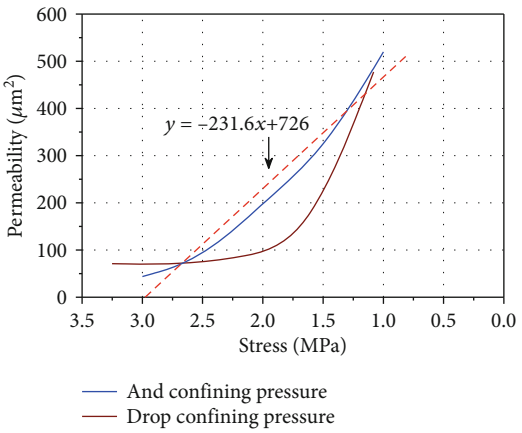

Figure 14: Permeability change curve of coal specimen under loading and unloading confining pressure.

The correlation coefficient of the trend line is $R^2 = 0.9754$ from the fitting result, and the data points are uniformly distributed at the two sides of the trend line. Hence, the change relationship between the rock permeability and confining pressure tends to be approximately linear after the confining pressure exceeds 1 MPa.

4.3. Gas Permeability of Prepeak Coal Specimen under First Unloading and Then Loading Confining Pressure. In view of the low permeability of prepeak rock, the coal specimen with favorable gas permeability is selected as the test specimen in the prepeak permeability test. Figure 14 shows the confining pressure-permeability curve.

The confining pressure is first unloaded and then loaded in this test. The confining pressure decreases from 3 to 1 MPa successively, then elevates from 1 to 3 MPa. The permeability change trend of the rock specimen is steady when the confining pressure started unloading from 3 to 2 MPa, but when the confining pressure is lower than 2 MPa, the permeability changes considerably. The permeability under 1 MPa is approximately five times that under 3 MPa, showing that the crack rapidly develops in the rock specimen when the confining pressure is unloaded from 2 to 1 MPa. The main reasons are as follows:

(1) During the unloading of confining pressure, the original cracks in the rock specimen expand and penetrate to form a seepage passage under the axial force

(2) From the stress state, before the rock specimen reaches the peak stress (approximate to peak stress), the rock specimen undergoes transverse deformation to form new cracks, and its permeability elevates due to the application of axial load during the unloading of confining pressure

(3) The confining pressure-permeability curve chart of the unloading of confining pressure was similar to that of the postpeak sandstone specimen, fully indicating that the rock clearly shows brittle characteristics under low confining pressure

(4) During the loading of confining pressure, the correlation coefficient of the trend line is obtained as $R^2 = 0.9811$ by fitting the confining pressure-permeability curve, manifesting the approximate linear change

5. Conclusions

The gas permeability values of prepeak and postpeak rock specimens are tested, and the following conclusions are drawn:

(1) The gas permeability of prepeak coal rock presents an approximately linear relation with confining pressure

(2) After the crack propagation in the postpeak rock reaches a stable state, the confining pressure gradually increases, and the gas permeability shows approximately under linear reduction; in the postpeak unloading phase, the opening and coalescence degree of rock cracks gradually extend the deformation, a seepage passage of well-interconnected cracks forms, and thus, the permeability reaches the peak value. Afterwards, in the strain softening phase, the cracks are closed to a certain extent, and thus, the permeability also decreases

(3) The unloading step size of confining pressure influences the gas permeability of coal and rock specimens: the smaller the unloading step size, the steadier the change of gas permeability becomes. The gas permeability of rock is greatly influenced by the confining pressure. Under low confining pressure, the gas permeability of postpeak rock has a very obvious turning point, which is generally within 0.5–1 MPa

Data Availability

The data used to support the findings of this study are available from the corresponding author upon request.

Conflicts of Interest

The authors declare that there is no conflict of interest regarding the publication of this paper.

Acknowledgments

This work is supported by the National Natural Science Foundation of China (No.51674007) and the Open Fund of "State Key Laboratory of Water Resource Protection and Utilization in Coal Mining" (SHJT-17-42.5).

References

[1] L. Yuan, "Theory and practice of integrated pillarless coal production and methane extraction in multiseams of low permeability," *Strategic Study of CAE*, vol. 11, no. 5, pp. 72–80, 2009.

[2] L. Yuan, "Strategic thinking of simultaneous exploitation of coal and gas in deep mining," *Journal of China Coal Society*, vol. 41, no. 1, pp. 1–6, 2016.

[3] L. Yuan, "Innovation and development of safety science and technology in coal industry of China," *Safety in Coal Mines*, vol. 46, Supplement1, pp. 5–11, 2015.

[4] B. G. Hurd, "A liquid-Freon permeameter," *Society of Petroleum Engineers Journal*, vol. 2, no. 1, pp. 18–20, 1962.

[5] F. T. Howell, C. J. Payne, and C. J. Bow, "A permeameter for investigating the passage of water through unfissured samples of permo-triassic sandstone," *Civil Engineering and Public Works Review*, vol. 3, pp. 261-262, 1972.

[6] D. Jasinge, P. G. Ranjith, and S. K. Choi, "Effects of effective stress changes on permeability of latrobe valley brown coal," *Fuel*, vol. 90, no. 3, pp. 1292–1300, 2011.

[7] C. Zhu, X. Xu, X. Wang et al., "Experimental investigation on nonlinear flow anisotropy behavior in fracture media," *Geofluids*, vol. 2019, Article ID 5874849, 9 pages, 2019.

[8] C. B. Jiang, G. Z. Yin, Q. X. Huang, and H. R. Si, "Experiment of deformation property and gas permeation of containing-gas coal under confining pressure unloading process," *Journal of China Coal Society*, vol. 36, no. 5, pp. 802–807, 2011.

[9] Z. Li, H. Liu, Z. Dun, L. Ren, and J. Fang, "Grouting effect on rock fracture using shear and seepage assessment," *Construction And Building Materials*, vol. 242, article 118131, 2020.

[10] Z. Li, H. Zhou, D. Hu, and C. Zhang, "Yield criterion for rock-like geomaterials based on strain energy and CMP model," *International Journal of Geomechanics*, vol. 20, no. 3, article 04020013, 2020.

[11] X. G. Liu, F. Gao, X. R. Li et al., "Experimental study on mechanical properties and gas permeation characteristics of raw coal sample with low gas permeability," *Journal of China University of Mining & Technology*, vol. 42, no. 6, pp. 911–916, 2013.

[12] Z. Li, S. Liu, W. Ren, Q. Zhu, Z. Dun, and J. Fang, "Multiscale laboratory study and numerical analysis of water-weakening effect on shale," *Advances In Materials Science And Engineering*, vol. 2020, Article ID 5263431, 14 pages, 2020.

[13] Y. S. Pan, H. Luo, Z. H. Li, Y. F. Zhao, and X. C. Xiao, "Experimental study on gas permeability and charge induction of gaseous coal rock under confined pressure unloading," *Chinese Journal of Rock Mechanics and Engineering*, vol. 34, no. 4, pp. 713–719, 2015.

[14] J. H. Atkinson, "Geotechnology: an introductory text for students and engineers," *Engineering Geology*, vol. 14, no. 4, pp. 286–286, 1979.

[15] E. P. Robertson and R. L. Christiansen, "Modeling laboratory permeability in coal using sorption-induced strain data," *SPE Reservoir Evaluation & Engineering*, vol. 10, no. 3, pp. 260–269, 2007.

[16] B. M. Shi, Q. X. Yu, and K. Wang, "Test research on coal seam penetrability dynamic changing law by far-distance protecting stratum mining," *Chinese Journal of Rock Mechanics and Engineering*, vol. 25, no. 9, pp. 1917–1921, 2006.

[17] Q. Meng, H. Wang, M. Cai, W. Xu, X. Zhuang, and T. Rabczuk, "Three-dimensional mesoscale computational modeling of soil-rock mixtures with concave particles," *Engineering Geology*, vol. 277, article 105802, 2020.

[18] M. Tu, N. B. Huang, and B. A. Liu, "Research on pressure-relief effect of overlying coal rock body unsing far distance lower protective seam exploitation method," *Journal of Mining & Safety Engineering*, vol. 24, no. 4, pp. 418–421, 2007.

[19] Y. Wu, J. Liu, D. Elsworth, X. Miao, and X. Mao, "Development of anisotropic permeability during coalbed methane production," *Journal of Natural Gas Science and Engineering*, vol. 2, no. 4, pp. 197–210, 2010.

[20] Y. Wu, J. Liu, D. Elsworth, Z. Chen, L. Connell, and Z. Pan, "Dual poroelastic response of a coal seam to CO_2 injection," *International Journal of Greenhouse Gas Control*, vol. 4, no. 4, pp. 668–678, 2010.

[21] G. Yin, C. Jiang, W. Wang, Q. X. Huang, and H. R. Si, "Experimental study of influence of confining pressure unloading speed on mechanical properties and gas permeability of containing gas coal rock," *Chinese Journal of Rock Mechanics and Engineering*, vol. 30, no. 1, pp. 68–77, 2011.

[22] L. Yuan, "Concept of gas control and simultaneous extraction of coal and gas," *China Coal*, vol. 36, no. 6, pp. 5–12, 2010.

[23] L. Yuan and J. H. Xue, "Key technology of pillars- less coal and gas simultaneous mining in low permeability seam group," *Coal Science and Technology*, vol. 41, no. 1, pp. 5–11, 2013.

[24] M. Yuan, J. Xu, B. Li, J. Cao, M. Zhang, and Y. T. Chen, "Experimental study of permeability and deformation of anthra cite during process of gaseous loading- unloading," *Chinese Journal of Rock Mechanics and Engineering*, vol. 33, no. 10, pp. 2138–2146, 2014.

[25] S. N. Zhou and B. Q. Lin, *The Theory of Gas Flow and Storage in Coal Seams*, China Coal Industry Publishing House, Xuzhou, China, 1998.